

High sub-bandgap response and fast switching enabled by thermal quenching in carbon-doped semi-insulating GaN

Jiahao Dong^{1,2}, Sanam SaeidNahaei¹, Austin Fehr¹, Auditee Majumder Momo³, Pramod Reddy³, Ronny Kirste³, Zlatko Sitar³, Ramón Collazo³, Selim Elhadj^{1,a}

¹) Seurat Technologies, Wilmington, Massachusetts 01887, USA

²) Department of Materials Science and Engineering, Massachusetts Institute of Technology, Cambridge, Massachusetts 02139, USA

³) Department of Materials Science and Engineering, North Carolina State University, Raleigh, North Carolina 27695, USA

^a) Corresponding author: elhadj@vt.edu

Abstract: Carbon-doped GaN is a promising material for sub-bandgap triggered optical switches. When incorporated in GaN, carbon introduces deep compensating centers that enable defect-mediated extrinsic photoconductivity. In this work, we investigate the optical responsivity and switching kinetics of semi-insulating carbon-doped GaN actuated by sub-bandgap blue illumination. A high ON/OFF ratio exceeding 10^7 is achieved under low-irradiance 405-nm photoexcitation. Temperature-dependent transient measurements reveal that the photocurrent decay kinetics follow a two-regime thermally activated behavior, with an activation energy of approximately 0.3 eV above the crossover temperature and near-zero activation energy below it. The two-regime behavior can be explained by a change of the dominant carrier recombination channel. We demonstrate that when heating above the crossover temperature, thermally induced quenching can accelerate the photocurrent decay by a factor of five, enabling significantly faster optical switching. The observed 0.3 eV activation energy may be associated with carbon-hydrogen defect complexes in GaN.

Carbon is one of the most important dopants in GaN, intentionally added or as an impurity. When incorporated during epitaxial growth, carbon can substitute on the nitrogen site, forming a deep acceptor C_N with a (0/-) transition approximately 0.9 eV above the valence band.^{1,2} This mid-gap state acts as an electron trap and compensates donors such as O or Si, rendering GaN semi-insulating.^{3,4} As a result, carbon is widely employed to suppress buffer leakage in nitride-based electronic devices.⁵⁻¹⁰

Despite its extensive use in buffer layers in nitride electronics, carbon-doped GaN has remained largely unexplored as an active optoelectronic layer. Carbon incorporation introduces mid-gap states that, in principle, enable defect-mediated photoconductivity and sub-bandgap optical switching. Similar mechanisms have enabled photoconductive semiconductor switches (PCSSs) in V-doped SiC, Ge-doped AlN, and N-doped diamond.¹¹⁻¹⁵ Yet, these material systems face practical limitations associated with epitaxial scalability and integration maturity. In contrast, C-doped GaN combines a mature epitaxial and processing ecosystem with well-established doping strategies, positioning it as a compelling but underexplored material for defect-engineered optical switching. More broadly, sub-bandgap photoresponse plays an important role in applications such as optically addressed spatial light modulators, photoelasticity and photoplasticity, and resistive switching.¹⁶⁻¹⁹

In this work, we investigate sub-bandgap photoresponse and optical switching kinetics in semi-insulating carbon-doped GaN. We demonstrate sub-bandgap optical switching with high ON/OFF ratio exceeding 10^7 at a low optical irradiance of 3.3 mW/cm^2 @ 405 nm. We systematically examine the temperature dependence of photoconductivity decay kinetics. In all carbon-doped samples tested, the decay kinetics exhibit two distinct thermally activated regimes, with an activation energy of approximately 0.3 eV above the crossover temperature (16 or 44 °C), and near-zero activation energy below it. This two-regime behavior can be explained by a change of the dominant carrier recombination channel: electron recapture at lower temperature, and hole-emission-assisted recombination at higher temperature. Notably, when heating above the crossover temperature, thermally induced quenching can accelerate the photocurrent decay by a factor of five. This suggests that higher temperature operation can effectively increase current switching speed in sub-bandgap-triggered GaN:C. With reference to literature reports, we tentatively assign observed 0.3 eV activation energy to carbon-hydrogen defect complexes in GaN.

GaN:C samples grown by two different techniques were investigated, as illustrated in **Fig. 1**. **Fig. 1a** shows a 1- μm -thick C-doped GaN epilayer grown by metal organic chemical vapor deposition (MOCVD) on a c-plane ammonothermal GaN substrate under N-rich conditions. The C-doped layer was deposited on a 1- μm undoped GaN buffer layer. Detailed growth parameters are reported elsewhere.²⁰ In this sample, carbon concentration and combined Si and O donor concentration are both approximately $3.0 \times 10^{16} \text{ cm}^{-3}$. **Fig. 1b** shows a 400- μm -thick free-standing C-doped GaN single crystal grown by hydride vapor phase epitaxy (HVPE). In this sample, the carbon concentration is $2.7 \times 10^{17} \text{ cm}^{-3}$, while the combined Si and O donor concentration is approximately $1.0 \times 10^{17} \text{ cm}^{-3}$. In both samples $[\text{C}] \geq [\text{Si}] + [\text{O}]$, and thus the Fermi level is expected to be pinned around the deep acceptor level $\text{C}_\text{N} (0/-)$,²¹ rendering the GaN semi-insulating as confirmed by electrical measurements.

For photoconductivity measurements and capacitance-voltage (C-V) profiling, vertical Schottky contacts were prepared on both samples: Ti/Al/Ti/Au was deposited on the bottom surface as ohmic contacts followed by rapid thermal annealing (RTA) at 950 °C for 30 s; Ni/Au (on the MOCVD GaN:C) or semitransparent Ni (on the HVPE GaN:C) contacts were deposited on the Ga-polar surface as Schottky contacts. On the HVPE GaN:C, the thin Ni layer has a thickness of 8 nm and 45% transmittance to 405 nm light.²² The semitransparent electrode enables calculation of optical responsivity. During testing of the photoresponse, the illumination was incident on the top Schottky contacts.

For steady-state photoluminescence (PL) analysis, the GaN:C samples were excited with a 325 nm continuous wave HeCd laser. The PL emissions were collected with a 0.75 m Acton SP2750 monochromator, and a PIXIS: 2KBUV cooled CCD camera. Samples were mounted in a helium flow cryostat, enabling low temperature PL measurements at 3 K. As shown in **Fig. 1c**, two dominant defect bands are observed in both samples: the yellow luminescence (YL) band with a maximum at $\sim 2.2 \text{ eV}$, and the blue luminescence (BL) band with a maximum at $\sim 3.0 \text{ eV}$. The YL band is associated with the $\text{C}_\text{N} (0/-)$ transition in C-doped GaN.^{1,4,21,23} The isolated C_N may also cause blue emission as a result of $(+ / 0)$ transition⁴ although recent analysis suggests that in highly-resistive GaN the BL band is related to the $\text{C}_\text{N}\text{H}_\text{i}$ complex.^{24–26} We summarize the possible main defect transitions expected for these samples in **Fig. 1d** as suggested by the PL spectra and literature reports.

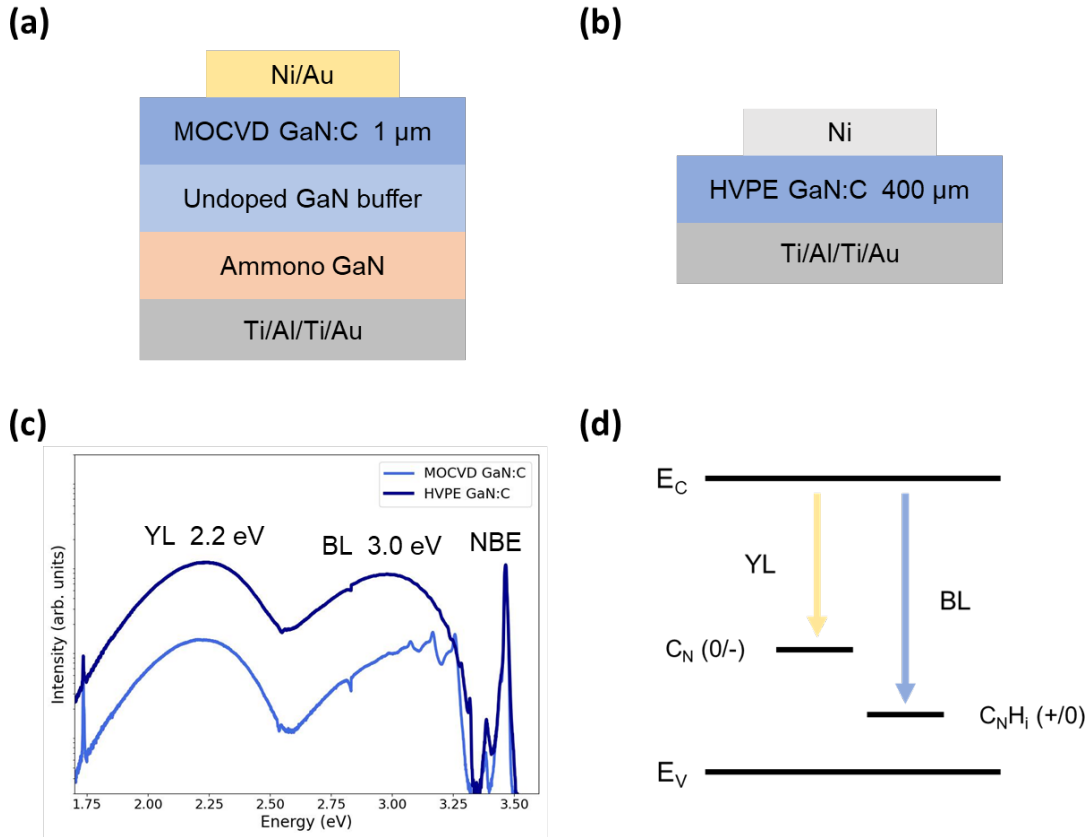


Figure 1: Structure of the GaN:C samples, steady-state PL spectra and proposed main defect transitions. (a) GaN:C as well as undoped GaN buffer layer grown with MOCVD on an ammonothermal GaN substrate, with Ni/Au deposited on the top as Schottky contact. (b) HVPE GaN:C with an 8-nm semitransparent Ni layer deposited on the top as Schottky contact. On both samples, Ti/Al/Ti/Au was deposited on the bottom surface as ohmic contacts. (c) Steady-state PL spectra for the GaN:C in (a) and (b) measured at 3 K. YL, BL and NBE represent yellow luminescence, blue luminescence, and near-band-edge emission, respectively. (d) Proposed main defect transitions in these GaN:C as suggested by the PL spectra in (c) and by comparison with literature reports.

Fig. 2 describes I-V measurements of the GaN:C samples under dark and under 405-nm excitation (Thorlabs SOLIS-405C), respectively. The photon energy of excitation is 3.06 eV, below the GaN bandgap (3.40 eV). The dark current is below 10^{-7} mA/cm², confirming that the samples tested here are semi-insulating. Under light, for the MOCVD GaN:C, an ON/OFF ratio of 10^7 is achieved at a forward bias of 1 V and a low irradiance of 3.3 mW/cm² @ 405 nm. For the HVPE GaN:C, an ON/OFF ratio of 10^9 is achieved at the same bias and irradiance. The measured I-V curves of both samples show rectifying characteristics, as expected for Schottky diodes. The HVPE GaN:C shows a higher leakage current under reverse bias, as expected from a higher dislocation density in the HVPE-grown crystal. Further, we estimate the sub-bandgap responsivity of the HVPE GaN:C is 3.3 A/W @ 405 nm, by using a transmittance of 45% for the thin nickel layer.

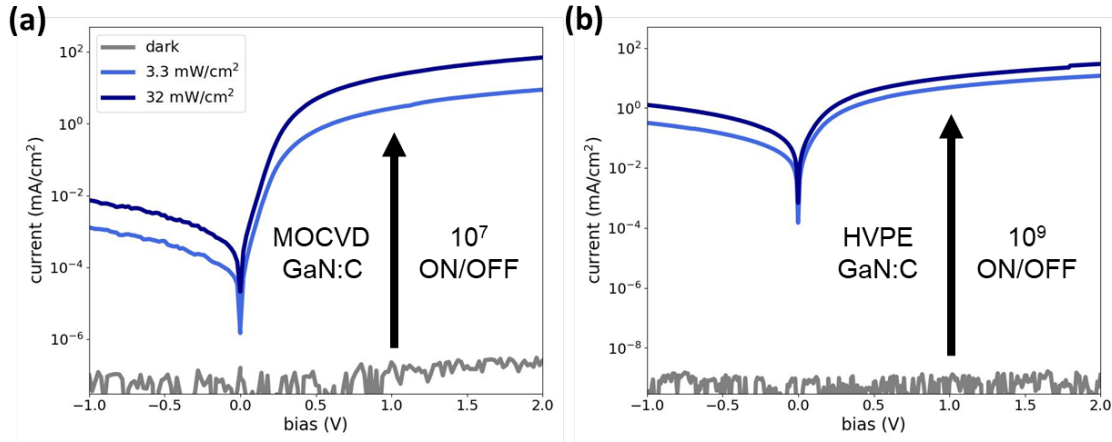


Figure 2: Measured I-V curves under dark and light, respectively. Bias was applied on the top Schottky contact. Current measured from -1 to 2 V under dark (grey line) and 405-nm illumination at various irradiance (blue lines) for (a) the MOCVD GaN:C and (b) the HVPE GaN:C.

To estimate the carrier concentration induced by sub-bandgap light, we measured C-V @ 100 kHz with an LCR meter (HIOKI 3533). Under dark, due to very low concentration of background carriers, we observed constant capacitance versus forward or reverse bias for both samples, consistent with previous reports on GaN doped with [C] > [Si].²⁷ Nonetheless, the sub-bandgap excitation can photoionize carbon-related defect centers and increase the *n*-type carrier concentration, enabling the extraction of the photocarrier concentration. Under 405-nm excitation of 32 mW/cm², we estimated a photocarrier concentration of 3.9×10^{16} cm⁻³ in the MOCVD GaN:C, and 2.5×10^{17} cm⁻³ in the HVPE GaN:C. These numbers are close to the nominal carbon doping concentration in both samples, suggesting that most of the carbon-related trap levels can be photoionized.

We performed transient photoconductivity measurements at various temperatures using a cryostat from Semetrol. The photocurrent transients enable the extraction of the current switching time—a key metric for optical switches—and the activation energies of the different underlying defect transitions. As shown in **Figs. 3a** and **3d**, transient photocurrent decay was measured at a forward bias of 2 V on both GaN:C samples from 194 to 394 K, after an optical pulse of 405-nm excitation @ 220 mW/cm² for 5 s. The photocurrent decay rates are extracted with a single-exponential fitting and summarized in the Arrhenius plots shown in **Figs. 3b** and **3e**. We note that a single exponential does not fully describe the decay kinetics; instead, it captures the dominant decay component that determines the effective turn-off time (<15 ms, as shown below). Notably, in both samples the photocurrent decay rates exhibit two distinct thermally activated regimes. The MOCVD GaN:C shows an approximately temperature-independent decay rate at low temperatures, followed by a thermally activated regime with an activation energy of 0.30 eV above a crossover temperature of 289 K (16 °C), as shown in **Fig. 3b**. Similarly, for the HVPE GaN:C, activation energies of 0.04 eV at low temperatures and 0.29 eV at high temperatures are observed, with a crossover temperature of 317 K (44 °C), as shown in **Fig. 3e**. This two-regime behavior indicates a change of the dominant recombination channel with increasing temperature. Importantly, the larger activation energy in the high-temperature regime suggests that the decay transients can be effectively quenched when heating above the crossover temperature. This motivates us to use higher temperature to reduce the turn-off time of the GaN:C optical switches. In **Figs. 3c** and **3f** we show 95% turn-off time (the time it takes for photocurrent to decay to 5% of the steady state value) as a function of

temperature for the two GaN:C samples. For the MOCVD GaN:C, increasing temperature from 20 °C (*i.e.*, room temperature) to 70 °C reduces turn-off time by 78% – from 9 to 2 ms. For the HVPE GaN:C, heating from 20 °C to 70 °C reduces turn-off time by 44% – from 9 to 5 ms. At the same temperature range, thermal quenching is more effective for the MOCVD GaN:C because of its lower crossover temperature.

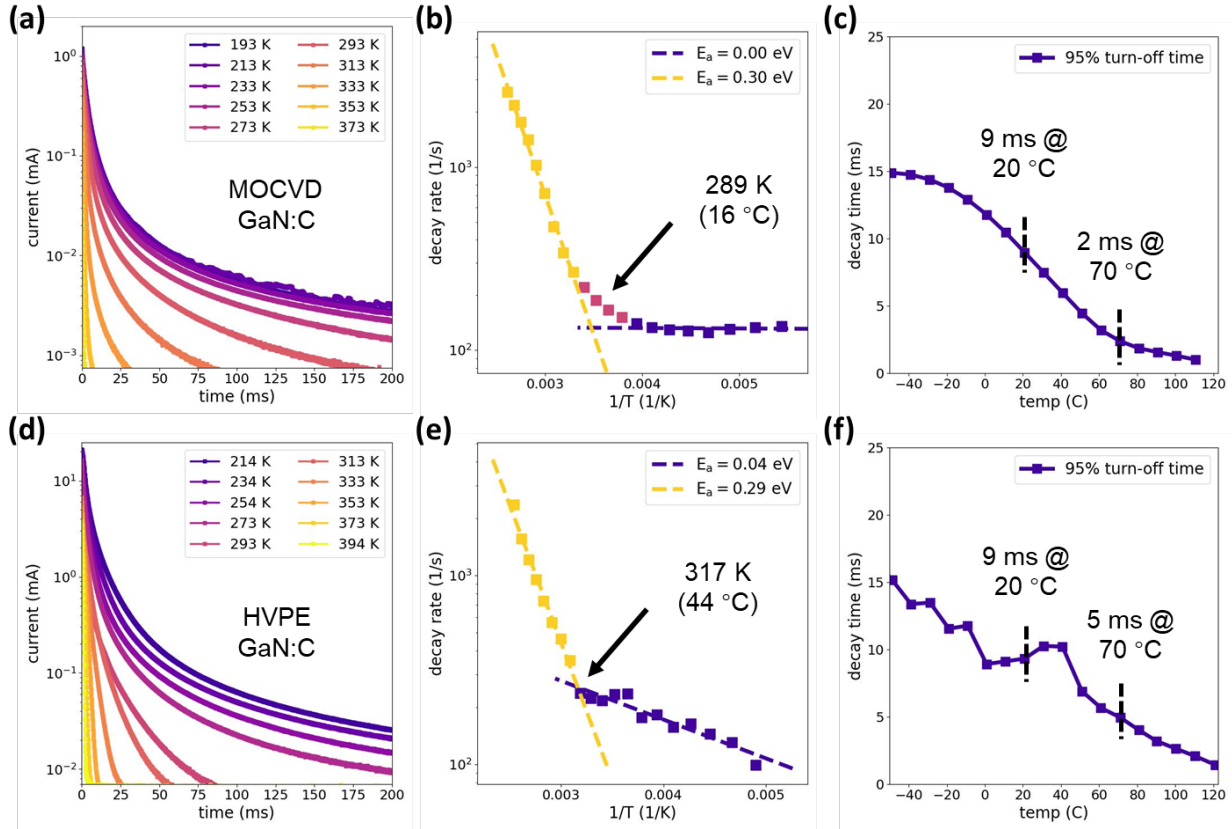


Figure 3: Photocurrent transients, Arrhenius plots and turn-off times. (a) Photocurrent transients after light turning off, (b) Arrhenius plot of decay rates and (c) 95% turn-off time for the MOCVD GaN:C. (d), (e) and (f) are the same plots for the HVPE GaN:C. Decay rates demonstrate two distinct regimes, which are plotted with different colors.

To compare with previously reported sub-bandgap optical switches, we summarize the optical switching performance of the GaN:C samples tested in this work in **Table I**. The GaN:C presented here compare favorably in terms of responsivity, ON/OFF ratio, and turn-off time. The sub-bandgap responsivity of the GaN:C is several orders of magnitude higher than the diamond:N, and slightly lower than the AlN:Ge. The strong optical response under sub-bandgap excitation allows effective triggering with visible light, eliminating the need for more hazardous ultraviolet (UV) light sources. Moreover, operation at elevated temperature significantly reduces turn-off time, enabling much faster current switching.

| Material | λ_{exc} (nm) | R (A/W) | $I_{\text{on}}/I_{\text{off}}$ | Turn-off time | Reference |
|-----------------|-----------------------------|--------------------|--------------------------------|---------------|--------------------|
| N-doped diamond | 532 | 7×10^{-5} | - | - | Ref. ¹³ |
| Ge-doped AlN | 455 | 18 | 10^5 | <100 ms | Ref. ¹² |

| | | | | | |
|---------------------|-----|-----|--------|--------------|-----------|
| C-doped GaN [MOCVD] | 405 | - | 10^7 | 2 ms @ 70 °C | This work |
| C-doped GaN [HVPE] | 405 | 3.3 | 10^9 | 5 ms @ 70 °C | This work |

Table I: Performance comparison of the GaN:C studied in this work with other sub-bandgap-triggered WBG and UWBG materials. λ_{exc} is the excitation wavelength for actuating the switch and R is the corresponding optical responsivity.

The two-regime activation of photocurrent decay kinetics suggests a change of the dominant defect recombination channel with increasing temperature, which we model in the schematic band diagrams in **Fig. 4**. Upon sub-bandgap excitation, carbon-related defects release electrons to the conduction band, rendering the GaN:C *n*-type. After light is turned off, decay of photocarriers can happen through two channels: electron recapture by the photoionized trapping centers as shown in **Fig. 4a**; hole-emission-assisted e-h recombination as shown in **Fig. 4b**. The electron recapture by trapping centers is barrierless, and therefore the transition rate is independent of temperature. In contrast, the hole emission is thermally activated, with a barrier height of $E_t - E_v$, where E_t is the trap level and E_v the valence band level. At elevated temperature, holes are emitted to the valence band from trap levels; these extra holes enable electron-hole recombination in all other channels (including radiative and nonradiative),²¹ thus accelerating decay of *n*-type carriers and photocurrent transients. Therefore, the 0.3 eV activation energy observed in the photocurrent quenching should be related to the hole emission barrier of a trap level at $E_v + 0.3$ eV.

The model in **Fig. 4** is consistent with the two-regime behavior we observed in the photocurrent decay: at low temperature ($T < T_C$ where T_C is the crossover temperature), the density of thermally ionized holes is negligible, and the photocarrier decay is dominated by electron recapture, which shows near-zero activation energy shown in **Fig. 3**; at high temperature ($T > T_C$), hole emission from the $E_t = E_v + 0.3$ eV trap level is activated and hole-emission-assisted e-h recombination become the dominant decay channel, giving rise to the 0.3 eV activation energy shown in **Fig. 3**. However, in HVPE GaN:C we observed a small yet nonzero activation energy of 0.04 eV at $T < T_C$, possibly because of existence of shallow donor states E_d (labeled in **Fig. 4**). Above the crossover temperature, both samples show almost the same activation energy, implying that the same trap level is thermally activated. The trap level observed in this work may be associated with the $C_N H_i$ (0/+) transition at around 0.3 eV above the valence band.²⁴

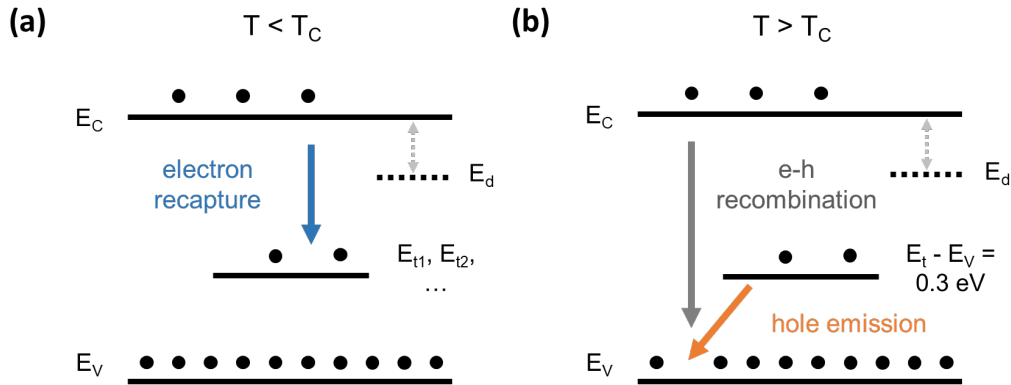


Figure 4: Modeling of the dominant recombination channels in the GaN:C samples after being excited with sub-bandgap light. (a) Electron recapture from the conduction band to photoionized trap levels when temperature is lower than the crossover temperature T_C . Electrons may be captured by multiple trap levels E_{t1}, E_{t2}, \dots E_C and E_V

are conduction and valence band levels, respectively. E_d represents possible existence of shallow donor states. (b) Hole-emission-assisted e-h recombination when temperature is higher than T_C . Holes are released to the valence band from the trap level at $E_t + 0.3$ eV, which then recombine with electrons in all other channels (including radiative and nonradiative, not drawn here).

The model shown in **Fig. 4** implies that the photocarrier decay rate is limited by the electron capture rate and $1/\tau_{ec}$ and hole emission $1/\tau_{he}$, which are given by the following equations:^{18,28}

$$\frac{1}{\tau_{ec}} = (N_t - n_t)v_{rms}\sigma_n \quad (1)$$

$$\frac{1}{\tau_{he}} = N_V v_{rms} \sigma_p \exp\left(-\frac{E_t - E_V}{k_B T}\right) \quad (2)$$

where N_t and n_t are the total and occupied electron trap concentrations, N_V the valence band density of states, and v_{rms} the carrier root mean square velocity. σ_n and σ_p are the apparent electron and hole capture cross sections, respectively. In principle, we can extract σ_n and σ_p using the photocurrent decay rates shown in **Fig. 3**, with the decay rate limited by $1/\tau_{ec}$ at $T < T_C$ and limited by $1/\tau_{he}$ at $T > T_C$. In practice, electrons in the conduction band may be captured by multiple trap levels in parallel (E_{t1} , E_{t2} , ...), which cannot be easily separated in photocurrent transients. Nonetheless, we can extract the hole capture cross section σ_p for the $E_V + 0.3$ eV trap level using Eq. (2), as summarized in **Table II**. The very low capture cross section values are consistent with the millisecond-scale photoconductivity decay observed in this work, indicating complex and slow decay dynamics.^{29,30} The underlying microscopic origin remains unresolved but may involve decay dynamics influenced by other trap states. Tentative assignment of the observed 0.3 eV activation energy to the $C_N H_i$ (0/+) transition level is shown in **Table II**. However, Reshchikov suggested that in semi-insulating GaN the apparent activation energy may be not related to the defect level.³¹ Thus, this assignment solely based on activation energy may not be definitive. Still, although the decay's microscopic origin is complex and specific to the materials growth conditions, the pronounced acceleration of current switching with increasing temperature clearly demonstrates that thermal activation plays a key role, offering a practical pathway towards faster photoconductive switching operation in C-doped GaN optoelectronic devices.

| Sample | HVPE GaN:C | MOCVD GaN:C |
|---------------------|------------------------------------|------------------------------------|
| σ_p | $2.6 \times 10^{-20} \text{ cm}^2$ | $7.6 \times 10^{-20} \text{ cm}^2$ |
| E_t | $E_V + 0.29 \text{ eV}$ | $E_V + 0.30 \text{ eV}$ |
| Possible assignment | $C_N H_i$ (+/0) | |

Table II: Defect parameters extracted from decay rates of photocurrent transients for both GaN:C samples. Tentative assignment to specific defect transition level is also shown.

In conclusion, we demonstrate that strong sub-bandgap response can be achieved in semi-insulating GaN with moderate carbon doping concentration. The GaN:C shows a high ON/OFF ratio of over 10^7 under low-irradiance blue illumination. Compared with previously reported sub-bandgap optical switches, the GaN:C presented here exhibit competitive optical responsivity, ON/OFF ratio, and switching speed. We examine the temperature dependence of photocurrent decay transients, and we found that thermal

quenching happens above a crossover temperature T_C (16 or 44 °C, depending on the sample) with an activation energy of 0.3 eV. Due to the thermal quenching, the optical switching speed is accelerated by about five times simply by heating the GaN:C from 20 to 70 °C. We attribute the observed thermal quenching to a change of the dominant recombination process, *i.e.*, from electron recapture at $T < T_C$ to hole-emission-assisted e-h recombination at $T > T_C$. The observed 0.3 eV activation energy in the photocurrent quenching may be related to a deep hole trap at $E_V + 0.3$ eV, which might be assigned to $C_N H_i (+/0)$. While the microscopic origin of the underlying defect transition requires further work to resolve, the significant acceleration of photoconductive switching with increasing temperature provides an important insight into achieving faster operation in GaN-based optoelectronic devices, and highlights the role of defect states in governing switching dynamics and material behavior at elevated temperatures.

References

- ¹ J.L. Lyons, A. Janotti, and C.G. Van De Walle, “Carbon impurities and the yellow luminescence in GaN,” *Appl. Phys. Lett.* **97**(15), 152108 (2010).
- ² J.L. Lyons, E.R. Glaser, M.E. Zvanut, S. Paudel, M. Iwinska, T. Sochacki, and M. Bockowski, “Carbon complexes in highly C-doped GaN,” *Phys. Rev. B* **104**(7), 075201 (2021).
- ³ D.S. Green, U.K. Mishra, and J.S. Speck, “Carbon doping of GaN with CBr₄ in radio-frequency plasma-assisted molecular beam epitaxy,” *J. Appl. Phys.* **95**(12), 8456–8462 (2004).
- ⁴ J.L. Lyons, A. Janotti, and C.G. Van De Walle, “Effects of carbon on the electrical and optical properties of InN, GaN, and AlN,” *Phys. Rev. B* **89**(3), 035204 (2014).
- ⁵ C. Poblenz, P. Waltereit, S. Rajan, S. Heikman, U.K. Mishra, and J.S. Speck, “Effect of carbon doping on buffer leakage in AlGaIn/GaN high electron mobility transistors,” *J. Vac. Sci. Technol. B Microelectron. Nanometer Struct. Process. Meas. Phenom.* **22**(3), 1145–1149 (2004).
- ⁶ Z.-Q. Fang, B. Claflin, D.C. Look, D.S. Green, and R. Vetury, “Deep traps in AlGaIn/GaN heterostructures studied by deep level transient spectroscopy: Effect of carbon concentration in GaN buffer layers,” *J. Appl. Phys.* **108**(6), 063706 (2010).
- ⁷ S.W. Kaun, M.H. Wong, J. Lu, U.K. Mishra, and J.S. Speck, “Reduction of carbon proximity effects by including AlGaIn back barriers in HEMTs on free-standing GaN,” *Electron. Lett.* **49**(14), 893–895 (2013).
- ⁸ A. Fariza, A. Lesnik, J. Bläsing, M.P. Hoffmann, F. Hörich, P. Veit, H. Witte, A. Dadgar, and A. Strittmatter, “On reduction of current leakage in GaN by carbon-doping,” *Appl. Phys. Lett.* **109**(21), 212102 (2016).
- ⁹ Ö. Danielsson, X. Li, L. Ojamäe, E. Janzén, H. Pedersen, and U. Forsberg, “A model for carbon incorporation from trimethyl gallium in chemical vapor deposition of gallium nitride,” *J. Mater. Chem. C* **4**(4), 863–871 (2016).
- ¹⁰ W. Cao, C. Song, H. Liao, N. Yang, R. Wang, G. Tang, and H. Ji, “Numerical simulation analysis of carbon defects in the buffer on vertical leakage and breakdown of GaN on silicon epitaxial layers,” *Sci. Rep.* **13**(1), 14820 (2023).
- ¹¹ T. He, T. Shu, H. Yang, M. Yi, F. Liu, J. Yao, L. Wang, and T. Xun, “Effect of Donor–Acceptor Compensation on Transient Performance of Vanadium-Doped SiC Photoconductive Switches Using 532-nm Laser,” *IEEE Trans. Electron Devices* **71**(7), 4275–4282 (2024).
- ¹² J. Dong, and R. Jaramillo, “A Junction Photoconductive Semiconductor Switch (J-PCSS) in AlN with Sub-Band Gap Responsivity and Accelerated Turn-Off Speed,” *IEEE Electron Device Lett.* **46**(6), 916–919 (2025).
- ¹³ D.L. Hall, L.F. Voss, P. Grivickas, M. Bora, A.M. Conway, P. Scajev, and V. Grivickas, “Photoconductive Switch with High Sub-Bandgap Responsivity in Nitrogen-Doped Diamond,” *IEEE Electron Device Lett.* **41**(7), 1070–1073 (2020).
- ¹⁴ E. Majda-Zdancewicz, M. Suproniuk, M. Pawłowski, and M. Wierzbowski, “Current state of photoconductive semiconductor switch engineering,” *Opto-Electron. Rev.* **26**(2), 92–102 (2018).
- ¹⁵ V. Meyers, L. Voss, J.D. Flicker, L.G. Rodriguez, H.P. Hjalmarsen, J. Lehr, N. Gonzalez, G. Pickrell, S. Ghandiparsi, and R. Kaplar, “Photoconductive Semiconductor Switches: Materials, Physics, and Applications,” *Appl. Sci.* **15**(2), 645 (2025).
- ¹⁶ S. Elhadj, Z. Davidson, and Y. Sargol, “A light-driven light valve for metal additive manufacturing,” in *Smart Mater. Opto-Electron. Appl.*, edited by I. Rendina, L. Petti, D. Sagnelli, and G. Nenna, (SPIE, Prague, Czech Republic, 2023), p. 3.
- ¹⁷ J. Dong, Y. Li, Y. Zhou, A. Schwartzman, H. Xu, B. Azhar, J. Bennett, J. Li, and R. Jaramillo, “Giant and Controllable Photoplasticity and Photoelasticity in Compound Semiconductors,” *Phys. Rev. Lett.* **129**(6), 065501 (2022).
- ¹⁸ J. Dong, and R. Jaramillo, “Modeling defect-level switching for nonlinear and hysteretic electronic devices,” *J. Appl. Phys.* **135**(22), 224501 (2024).

- ¹⁹ B. Chatterjee, S. Ghandiparsi, M.S. Gottlieb, Q. Shao, C.D. Frye, S. Harrison, and L. Voss, “Wide bandgap photoconductor (SiC:V)-based optically addressed light valve for high fluence operation,” *Appl. Opt.* **64**(10), 2324 (2025).
- ²⁰ S. Rathkantiwar, P. Bagheri, D. Khachariya, S. Mita, S. Pavlidis, P. Reddy, R. Kirste, J. Tweedie, Z. Sitar, and R. Collazo, “Point-defect management in homoepitaxially grown Si-doped GaN by MOCVD for vertical power devices,” *Appl. Phys. Express* **15**(5), 051003 (2022).
- ²¹ M.A. Reshchikov, M. Vorobiov, D.O. Demchenko, Ü. Özgür, H. Morkoç, A. Lesnik, M.P. Hoffmann, F. Hörich, A. Dadgar, and A. Strittmatter, “Two charge states of the C_N acceptor in GaN: Evidence from photoluminescence,” *Phys. Rev. B* **98**(12), 125207 (2018).
- ²² M.A. Nasiri, A. Seijas-Da Silva, J.F. Serrano Claumarchirant, C.M. Gómez, G. Abellán, A. Cantarero, and J. Canet-Ferrer, “Ultrathin Transparent Nickel Electrodes for Thermoelectric Applications,” *Adv. Mater. Interfaces* **11**(5), 2300705 (2024).
- ²³ S.G. Christenson, W. Xie, Y.Y. Sun, and S.B. Zhang, “Carbon as a source for yellow luminescence in GaN: Isolated CN defect or its complexes,” *J. Appl. Phys.* **118**(13), 135708 (2015).
- ²⁴ D.O. Demchenko, I.C. Diallo, and M.A. Reshchikov, “Hydrogen-carbon complexes and the blue luminescence band in GaN,” *J. Appl. Phys.* **119**(3), 035702 (2016).
- ²⁵ S. Wu, X. Yang, Q. Zhang, Q. Shang, H. Huang, J. Shen, X. He, F. Xu, X. Wang, W. Ge, and B. Shen, “Direct evidence of hydrogen interaction with carbon: C–H complex in semi-insulating GaN,” *Appl. Phys. Lett.* **116**(26), 262101 (2020).
- ²⁶ M.A. Reshchikov, O. Andrieiev, M. Vorobiov, B. McEwen, S. Shahedipour-Sandvik, D. Ye, and D.O. Demchenko, “Stability of the C_N H_i Complex and the Blue Luminescence Band in GaN,” *Phys. Status Solidi B* **258**(12), 2100392 (2021).
- ²⁷ C.H. Seager, A.F. Wright, J. Yu, and W. Götz, “Role of carbon in GaN,” *J. Appl. Phys.* **92**(11), 6553–6560 (2002).
- ²⁸ K. Decock, P. Zabierowski, and M. Burgelman, “Modeling metastabilities in chalcopyrite-based thin film solar cells,” *J. Appl. Phys.* **111**(4), 043703 (2012).
- ²⁹ M. Kato, T. Asada, T. Maeda, K. Ito, K. Tomita, T. Narita, and T. Kachi, “Contribution of the carbon-originated hole trap to slow decays of photoluminescence and photoconductivity in homoepitaxial n-type GaN layers,” *J. Appl. Phys.* **129**(11), 115701 (2021).
- ³⁰ N. Modolo, C. De Santi, A. Minetto, L. Sayadi, G. Prechtel, G. Meneghesso, E. Zanoni, and M. Meneghini, “Trap-state mapping to model GaN transistors dynamic performance,” *Sci. Rep.* **12**(1), 1755 (2022).
- ³¹ M.A. Reshchikov, N.M. Albarakati, M. Monavarian, V. Avrutin, and H. Morkoç, “Thermal quenching of the yellow luminescence in GaN,” *J. Appl. Phys.* **123**(16), 161520 (2018).